Extending the Mathews stability graph for open-stope design

C. Mawdesley, R. Trueman and W. J. Whiten

Synopsis

The Mathews method of predicting open-stope stability was first proposed in 1980. The initial stability graph was based on a limited number of case studies, primarily from deep, North American, steeply dipping open stopes in strong rocks of medium to good quality. Since then new data have been added by various practitioners to modify, update and validate the method and support its use as a preliminary open-stope design tool.

The original Mathews method has been extended with use of a significantly increased database of mining case histories. The format of the Mathews stability graph has been changed to reflect the broader range of stope geometries and rock mass conditions now captured within the database. The extended database now contains in excess of 400 case histories.

Logistic regression has been performed on this larger database to delineate and optimize placement of the stability zones statistically. Isoprobability contours have been generated for all stability outcomes. The advantage of the logistic regression lies in its ability to minimize the uncertainties reflected in the method through the use of maximum likelihood estimates. The risks associated with use of the Mathews method can now be quantified and the true statistical significance of the stability zones understood.

Mathews stability graph method

The Mathews method[1] is based on a stability graph relating two calculated factors: the Mathews stability number, N, which represents the ability of the rock mass to stand up under a given stress condition; and the shape factor, S, or hydraulic radius, which accounts for the geometry of the surface.

The principal concept behind the stability graph is that the size of an excavation surface can be related to the rock mass competency to give an indication of stability or instability. The stability graph presents numerous excavation surfaces that have a specified range of stabilities. The stability number forms the y-axis of the stability graph and is a measure of rock mass quality around the excavation, several adjustments being applied to take into consideration induced stresses and excavation orientation.

Stability graphs deal with the individual surfaces of an excavation rather than entire excavations. For a typical rectangular excavation five stope surfaces are considered for the stability graph—four sidewalls and the crown (or back). Once plotted the stability data can be zoned and boundary lines can be drawn on to the graph to define the stability zones.

The initial stability zones and graph devised by Mathews were based on 50 case histories.[1] The zones of stability were defined from the scatter of the real mining data and these zones were then used to predict the stability of planned excavations. The original Mathews stability graph was divided into stable, potentially unstable and potential caving zones according to the scatter of the stability data (Fig. 1). The three stability zones were separated by transitional zones to reflect the transition between stability classes and uncertainty in the boundaries.

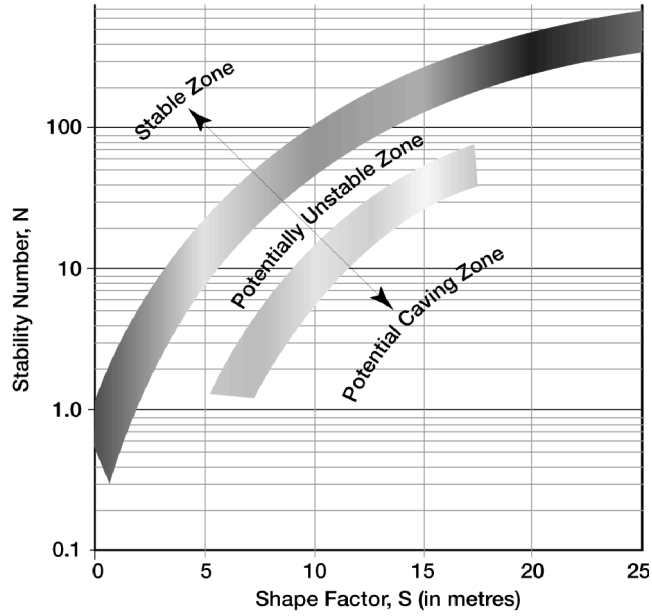

Fig. 1 Three stability zones of original Mathews stability graph. After Stewart and Forsyth[8]

The Mathews method utilizes a modified form of the Norwegian Geotechnical Institute's (NGI) engineering classification,[2] the Q system, to characterize rock mass quality. The modified Q value, Q', is calculated from the results of structural mapping or geotechnical core logging of the rock mass according to the Q classification system, but with the assumption that the joint water reduction parameter and the stress reduction factor are both equal to one (equation 1). The quality of the rock mass is defined by

$$Q' = \frac{\mathrm{RQD}}{\mathcal{J}_\mathrm{n}} \times \frac{\mathcal{J}_\mathrm{r}}{\mathcal{J}_\mathrm{a}} \qquad (1)$$

where RQD is the rock quality designation index developed by Deere in 1964 and is based on a modified core recovery percentage,[3] $\mathcal{J}_\mathrm{n}$ is joint set number, $\mathcal{J}_\mathrm{r}$ is joint roughness and $\mathcal{J}_\mathrm{a}$ is joint alteration.

The Mathews stability number is determined by adjusting the Q' value for induced stresses, discontinuity orientation and the orientation of the excavation surface (equation 2). The stability number is defined as

$$N = Q' \times A \times B \times C \qquad (2)$$

Manuscript first received by the Institution of Mining and Metallurgy on 7 February, 2000; revised manuscript received on 22 August, 2000. Paper published in *Trans. Instn Min. Metall.* (*Sect. A: Min. technol.*), **110**, January–April 2001.

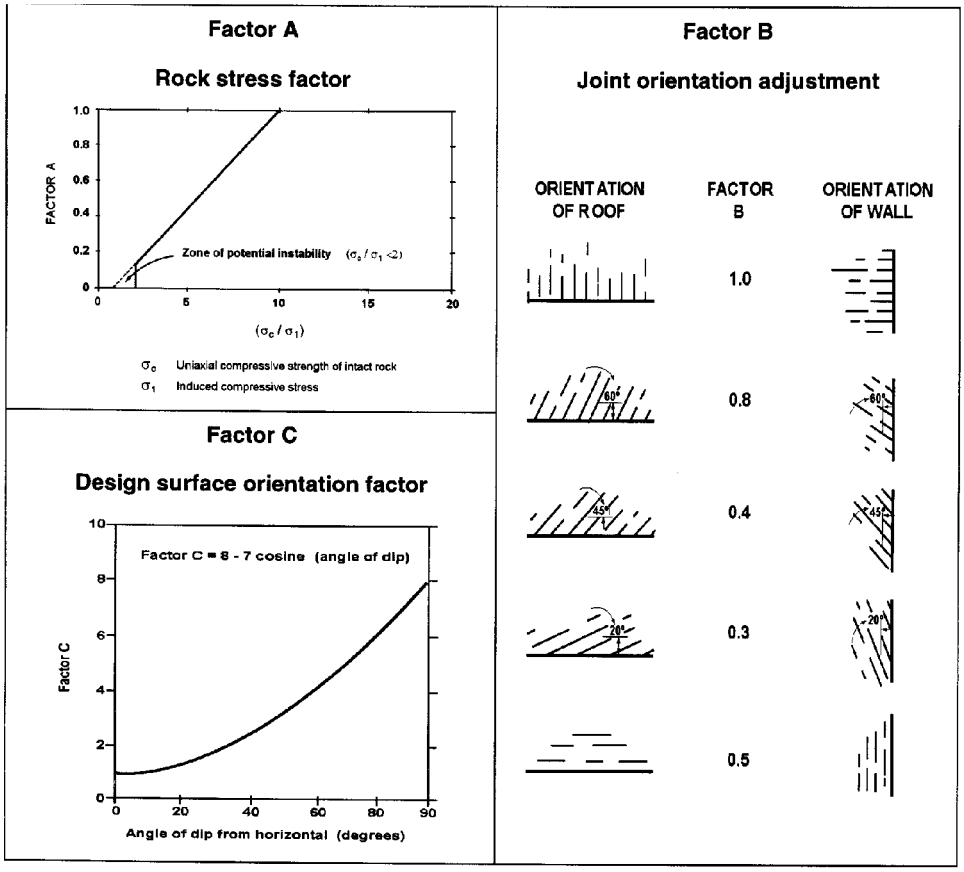

Fig. 2 Adjustment factors for determination of Mathews stability number. After Mathews *et al.*[1]

where Q' is NGI modified Q value, A is rock stress factor, B is joint orientation adjustment factor and C is surface orientation factor.

The rock stress factor is determined from the ratio of the intact rock strength (unconfined compressive strength) to the induced compressive stress at the centre-line of the stope surface. The induced stresses can be determined by use of a two-dimensional stress–displacement analysis package or estimated from published two-dimensional stress distributions. A graph relating the strength to stress ratio and rock stress factor was developed by Mathews *et al.*[1] (Fig. 2). In the original Mathews graph[1] the joint orientation adjustment factor is a measure of the relative difference in dip between the stope surface and the critical joint set. The surface orientation factor considers the inclination of the excavation surface and its influence on stability (Fig. 2).

The geometry of the excavation is considered by calculating the shape factor or hydraulic radius of the surface. The shape factor of an excavation surface is defined as the area of the stope surface divided by the length of its perimeter (in metres).

Historical overview

The Mathews stability graph method for open-stope design was first proposed for mining at depths below 1000 m.[1] A number of authors have since collected new data from a variety of mining depths and rock mass conditions to extend the method and test its validity.[4–9] The modifications to and developments of the Mathews method since its inception relate largely to changes in the position and number of the stability zones represented on the stability graph with the addition of more data and changes to the formulation of the Mathews factors.[9]

The original Mathews graph contained three distinct zones separated by transitions.[8] In the Potvin[4] modified stability graph the number of zones was reduced to a stable and a caved zone separated by a transition (Fig. 3). The choice of the word 'caved' by Potvin to represent what is essentially an unstable zone was challenged by Stewart and Forsyth,[8] who noted that the term has a fixed meaning in mining terminology from which Potvin's modified graph appears to depart.[8]

Potvin[4] collected additional case histories and modified the

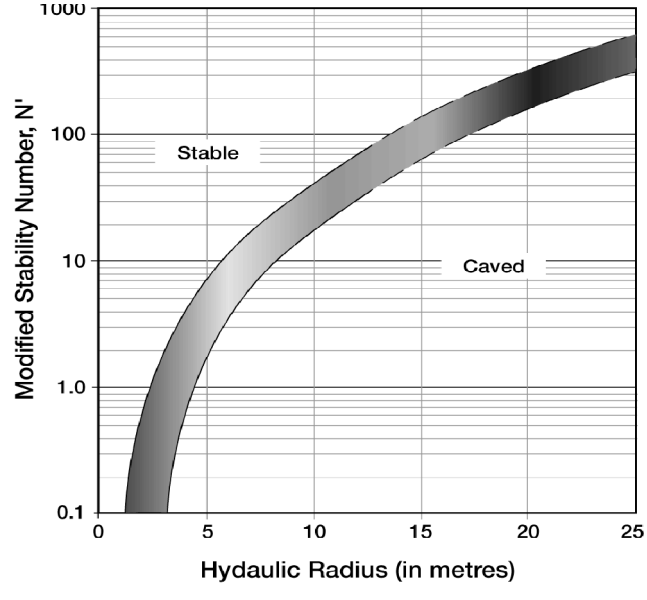

Fig. 3 Potvin's modified Mathews stability graph based on 175 case histories. After Potvin[4]

way in which the joint orientation factor and the gravity adjustment factor were calculated. This variant of the original Mathews method is referred to as Potvin's modified stability graph method. Potvin also extended the method to consider supported excavations, a development that was taken further by Nickson.[5] Nickson[5] and Hadjigeorgiou and co-workers[6] added further supported and unsupported case histories to the stability database using Potvin's modified method and were the first to consider statistical zone definition.

Stewart and Forsyth[8] updated the Mathews stability graph in 1995 and proposed four stability zones—potentially stable, potentially unstable, potential major failure and potential caving zones—separated by three transitions (Fig. 4). The zone of potential caving approximated by Stewart and Forsyth was based on Laubscher's caving stability graph.[10] No data were available to validate the position of the caving line on the updated Mathews graph, which is meant to represent the true caving situation, as opposed to Potvin's caved zone.[4] As part of an international study of block and panel caving, the authors have back-analysed a number of caving case histories and delineated a caving zone on the Mathews graph that reflects the true caving case defined as continuous cave propagation. At this stage the results remain confidential to sponsors of the project.

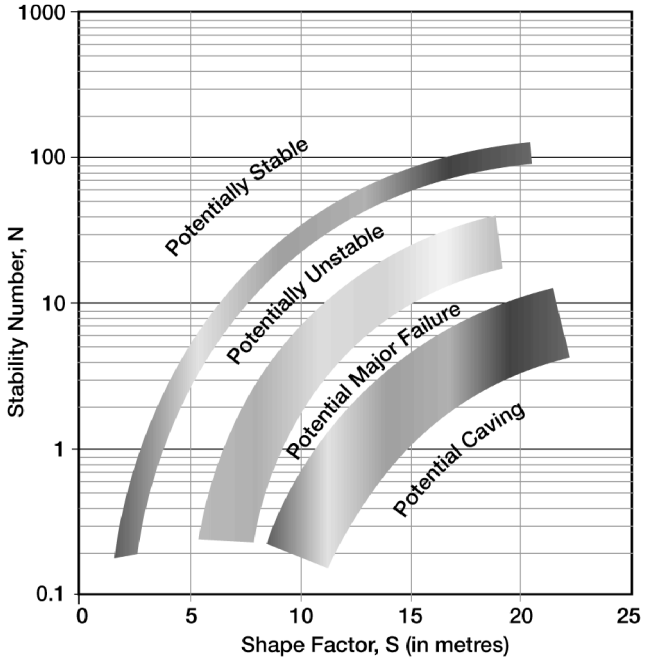

Fig. 4 Mathews stability graph as modified by Stewart and Forsyth[8]

Significant developments and modifications have been made to the stability graph method, extending its use into cable-supported excavations[4–7] and, more recently, to take account of fault-driven instability.[11] Potvin's modified approach, as applied to unsupported stopes, was compared with the original Mathews method for 180 case histories from Mt. Charlotte.[9] The variability of the results, the apparent predictive accuracy and the accuracy of the defined stability zones (in terms of misclassification) of the two methods were investigated. From these case studies Trueman *et al.*[9] concluded that Potvin's modifications to the method of calculating the stability number resulted in no appreciable difference in the predictive capability of the technique for unsupported excavations—a conclusion that was in general agreement with that of Stewart and Forsyth.[8] The original method of determining the Mathews stability number and the adjustment factors, as proposed by Mathews *et al.*,[1] has therefore been followed here.

Historically, the stability zones on the Mathews graph have been defined by eye.[1,4] As new data were added the nature and placement of the stability zones were modified accordingly. Nickson[5] was the first to attempt to determine the position of the boundaries statistically. He applied a discriminant analysis to the three-dimensional multivariate stability database and utilized Mahalanobis' distance to separate the data into two groups. Nickson derived a linear separation between stable and caved unsupported histories using a logarithmic transformation. Again, it should be noted that the term 'caved' does not represent true caving. No unstable cases were considered in the analysis and separation lines between stable and unstable or unstable and caving zones were not determined. Nickson compared his statistically determined stable–caved boundary with Potvin's proposed transition zone. Nickson recommended on the basis of his results that Potvin's transition zone be used for the design of unsupported stope surfaces. Hadjigeorgiou and co-workers[6] collected further stability data, repeated the discriminant analysis and obtained similar results. Again, no changes to Potvin's transition zone were proposed. The transition case histories were not included in either statistical analysis and the calculated boundary was only between the stable and caved case histories.

The position of the stability zones on the stability graph is critical to the reliability of the method and a technique was sought to optimize their positioning. Mathematical calculation of the width and position of the stability zones is an important step towards improving the reliability of the Mathews method. Removal of the subjectivity involved in zone definition is important in maximizing the value of the method as a design tool.

Extension of the Mathews method

Back-analyses of 180 open-stope surfaces at Mt. Charlotte by the Mathews method confirmed the validity of using the technique as a predictive tool.[9] These data, when combined with other Australian case histories in 1998, resulted in a combined stability database for more than 400 stope surfaces. The additional case histories included much larger stopes than had previously been documented for the method and they extend the Mathews graph to a hydraulic radius of 55 m, compared with the previous maximum hydraulic radius of 23 m.[8] The expanded database covers a broader spectrum of rock mass and *in-situ* stress conditions, with stability numbers in the range from 0.005 to 700. The background to the Mt. Charlotte data has already been given by Trueman *et al*;[9] the purpose of the present contribution is to communicate a new approach for the statistical treatment of stability data and for the calculation of stability zones and isoprobability contours on stability graphs.

A logistic regression analysis[12] was carried out on the extended database to delineate the zones of stability statistically and to determine isoprobability contours for stable, minor failure and major failure scenarios. All the case histories adhere to the original Mathews method of determining the adjustment factors. By the use of logistic regression the uncertainties in the application of the Mathews method can be quantified over a larger range of stope geometries and rock mass conditions than was previously possible. The extended Mathews stability graph (Fig. 5) contains the new data and statistically determined stability zones. A log–log graph has been used rather than the traditional log–linear plot of the Mathews method as it was found to give a clearer picture of the zoning. The log–log plot has linear stability boundaries

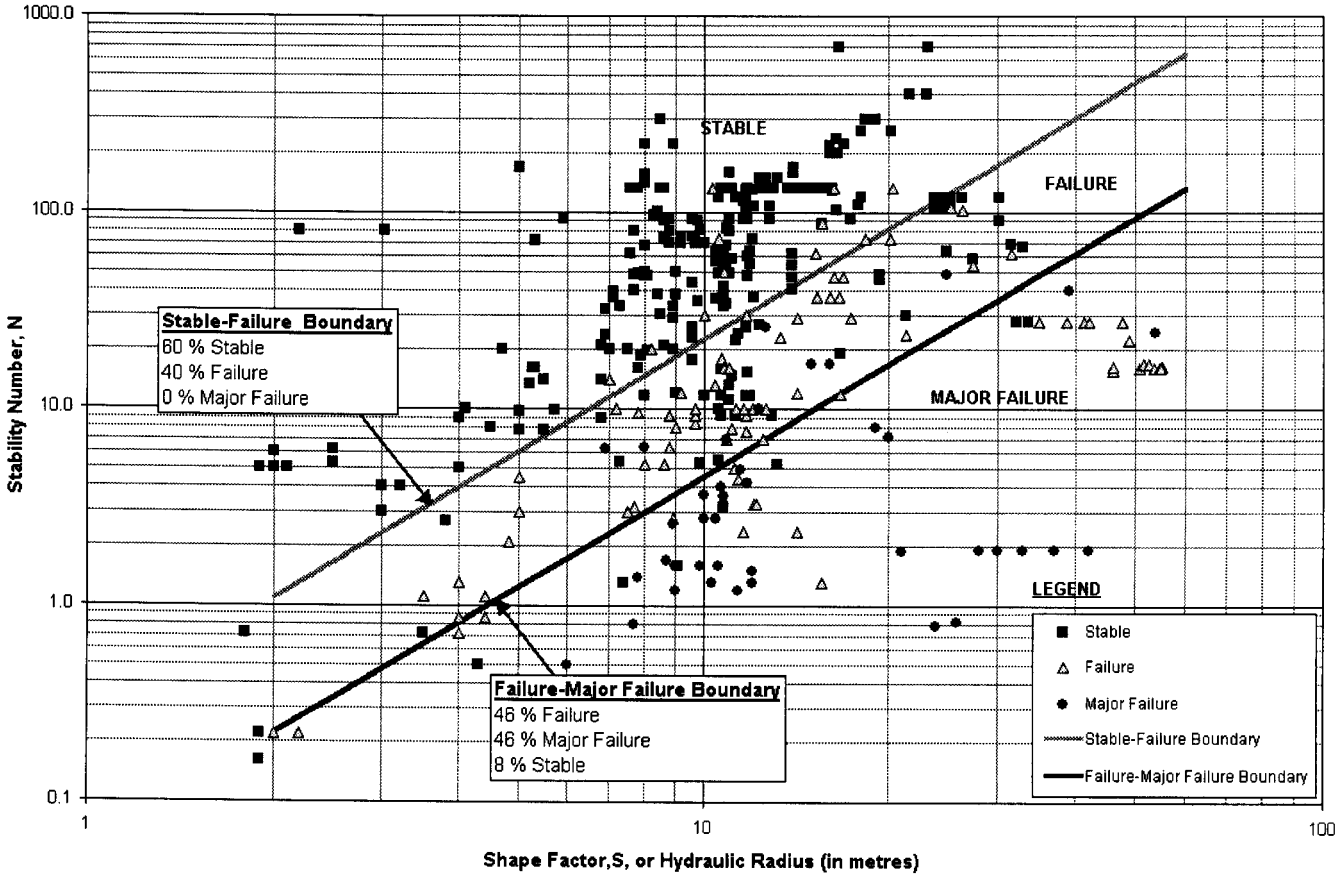

Fig. 5 Extended Mathews' stability graph based on logistic regression

and the shape factor range of the case histories is separated better on a log shape factor *x*-axis. The new log–log stability graph enables individual cases to be clearly distinguished as well as presents the increased range of shape factors captured within the stability database.

Logistic regression analysis

Logistic regression[12] provides a method of calculating the probability that a particular stope of a given dimension and geometry will be stable. It also shows how the probability of stability is altered by a change in rock mass quality or induced stress. The regression analysis allows statistical definition of the different zones of stability by optimizing the number of data points that report to the correct zones and minimizing misclassification.

Logistic regression analyses are typically used to analyse true or false values of the dependent variable, but can easily be extended to include estimates of the proportion true/false. A logistic regression analysis was undertaken because problems with ordered outcomes are not easily modelled by traditional regression techniques and ordinary linear regression does not consider the interval nature of the dependent variable.[13]

The stability data were specified in terms of three variables: shape factor (or hydraulic radius), Mathews stability number and stability (whether it was stable, a failure or a major failure). Logistic regression of these values fits a maximum likelihood model, calculates a separation line of best fit and produces a predicted stability value. The maximum likelihood method is used to maximize the value of the log-likelihood function by estimating the value of the parameters. Determination of the maximum likelihood estimates for the logistic regression model is an iterative process.[12] The stability data do not separate perfectly into each stability zone and, hence, the actual values of the dependent variable (stability) differ from the logit values. The logit probability values are used to optimize the boundaries of the three stability zones on the stability graph. The predicted stability values can be compared with the original values and the nature of the residuals can be analysed to delineate the stability zones and to consider misclassification.

One of the benefits of logistic regression is that it provides the predicted probabilities of event occurrence based on the logit model. By using the predicted probabilities of event occurrence calculated for each stability class isoprobability contours of risk can be generated for the stability data. Isoprobability contours are an important component of the Mathews stability graph method as they represent the estimated probability of event occurrence on the stability graph.

Logit model

Several models can be applied to the data when logistic regression is undertaken. For the stability data a modified binary logit model was used in which the logit function is a type of probability distribution.[13] For the interpretation of probabilities the logit model is more appropriate than the traditional linear model given by ordinary least squares.[12,13,14] Logit analysis produces probabilities after a nonlinear transformation for a categorical response; for the stability data two main discrete categories can be identified (stable and major failure)[14] and in-between probability values can be interpreted as the failure zone. The logit probability value is the natural logarithm of the odds, where the odds indicate the relative probability of falling into one or two categories on some variable of interest.[14] The logit model of the stability data was produced in MATLAB (version 5.1) using a routine developed by Holtsberg.[15] The regression procedure enabled the optimization of the stability zone boundaries and the gen-

eration of isoprobability contours by use of the predicted logit probability values determined from the logit model.

A three-level logit model was used in the investigation of the Mathews stability data to reflect the three stability classes. Logit models are typically applied to yes/no outcomes (giving a binary model), but for the present analysis a third, intermediate, category was used. The three-level logit model produced two separation lines between the three stability classes. The fact that the two lines were parallel is a function of the three-level model. The use of a three-level logit model to investigate the stability data was verified by running dual binary logit models to determine the stable–failure and the failure–major failure boundaries separately. These boundaries were found to be very close to parallel.

For a binary logit model the dependent variable is assigned a value of either zero or one. With three separate stability categories an intermediate value needed to be determined. A value of 0.5 was used for the failure region, which was considered intermediate between stable and major failure. The logit model was run for different values of the dependent variable categories and the distribution of the logit values so obtained was examined closely to consider overlap and spacing between the stability classes. The values assigned to each stability class as a result are: stable, 0.6–1; failure, 0.4–0.6; and major failure, 0–0.4.

Initial values of 1, 0.5 and 0 were used to define the three stability categories and for each point a logit probability value was calculated. The boundaries between the stability classes can then be determined at an appropriate probability for given site conditions or design requirements. Alternatively, given the equal probability lines, actual counts of the number of points in each class can be made, giving a distribution of points versus the probability value. A graph of these results is a useful way of determining the stability zone boundaries.

The inclination, position and probabilities of the two boundaries determined from the two separate binary logit models were compared with the two boundaries determined from the single three-level logit model. The observed differences in the position and inclination of the boundaries were minor and the three-level model was adopted.

The general form of the logit function can be seen in equation 3. The logit model is similar to the traditional linear regression model, or the general linear model for ANOVA, except that the response is the log odds rather than the metric dependent variable.[14] In logit modelling the conditional log odds of the dependent variable are expressed as a linear function of a set of explanatory variables (equations 3 and 4).[14] In the logit model of the stability data the probability of stability is expressed as a linear function of the shape factor, the Mathews stability number and a constant (equation 5).

To fit the logit model the unknown parameters α, β_1, β_2 … β_k (in equation 3) are estimated by the maximum likelihood method. With the use of the estimated values for α, β_1 and β_2 (equation 5) the estimated probability or predicted risk can be determined (equation 4). The general form of the logit function is

$$z = \alpha + \beta_1 X_1 + \beta_2 X_2 + \beta_3 X_3 + \ldots + \beta_k X_k = \alpha + \Sigma \beta_k X_k \quad (3)$$

$$f(z) = \frac{1}{\left(1 + e^{-z}\right)} \quad (4)$$

where z is predicted log odds value, α is a constant, $\beta_{1,2}$ are numerical coefficients and $f(z)$ is predicted logit probability value. For the case of open-stope stability equation 3 becomes

$$z = \alpha + \beta_1 \ln S + \beta_2 \ln N \quad (5)$$

The maximum likelihood statistic is used to define the inclination of the stability zone boundaries. By examination of the cumulative and probability density functions of the logit values for each class the position of the lines delineating each of the stability zones can be optimized according to the needs of particular applications. The criteria used to place the zones can be specified and the resulting probabilities for each stability class will then be known. By using the cumulative density functions for each class as determined in Fig. 7 the position of the stability zones can be optimized for certain criteria—for example, minimized misclassification (either numerically or proportionally) or, similarly, a more conservative limit of zero misclassification. This method is a significant improvement on earlier methods of delineating stability zones in that the probable stability outcomes for a boundary at *any* position of the stability graph can be quantified statistically. The probability density functions provide data on the degree of misclassification of the stability data, which is an important consideration

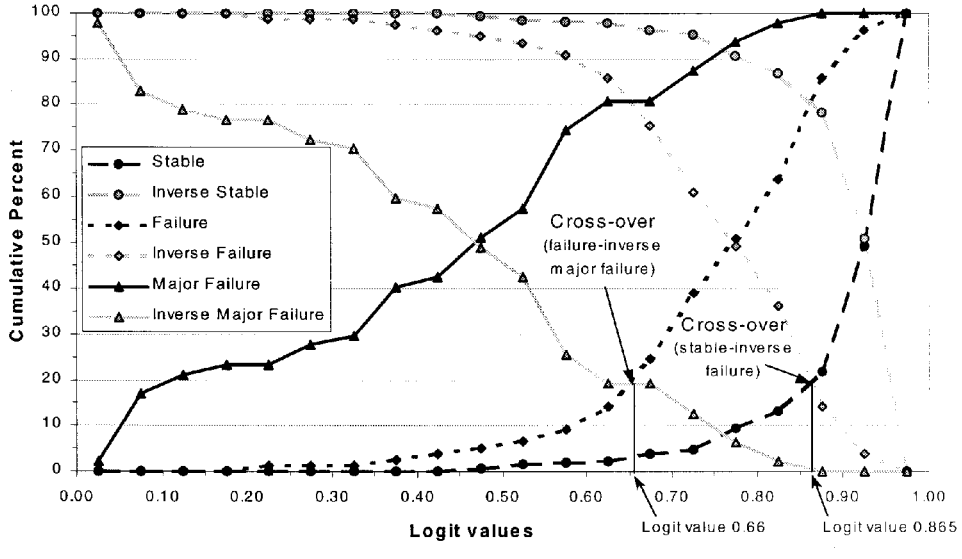

Fig. 6 Cumulative frequency graph of logit values for stable, failure and major failure points

when evaluating the confidence of a stability estimate and the potential for misclassification.

Delineation of stability zones

A cumulative distribution curve can be plotted for the logit probability values of the data for each stability class (Fig. 6). The inverse cumulative distribution curve of each class is also plotted. The point of intersection of the stable line and the inverse failure line is termed the crossover point. The crossover points on the cumulative distribution graph represent the logit probability value that will define the separation line that will have the same proportion of misclassified points on either side of the line. The cumulative frequency graph in Fig. 6 shows that for a logit probability of 0.865 there is a 20% mismatch of stable and failure cases. This means that 20% of the stable points lie below the separation line defined by a logit value of 0.865 (in either the failure or the major failure zone) and 20% of the failures lie above the line in the stable zone.

The true significance of the stable–failure line can be determined from the probability density functions for each stability class shown in Fig. 7. On the stable–failure boundary, with a logit value of 0.865, there is 48% probability of both stable conditions and failure and a 4% probability of a major failure. This can be directly converted into misclassification proportions, i.e. if a designed surface classed as stable plotted exactly on the line, there is a 52% probability that it would be a failure or major failure, i.e. would have been misclassified.

The positions of the separation lines on the stability graph were determined from the logit value at the crossover points on the cumulative frequency plots. Data of the type used here, originating from multiple sources, typically include the possibility of outliers. The location of outliers needs to be considered because the optimized location of the boundary obtained from the cumulative plot does not specifically consider the distribution of the outliers within the other stability zones. If a slight shift in the stable boundary would remove a significant number of failure points from the stable zone for a correspondingly lower number of stable points moving into the failure zone, a better boundary could exist than the optimized one indicated by the cumulative crossover logit value. The accuracy of the model can be assessed through significance testing, goodness-of-fit measures and by considering the magnitude of the residuals. Measures that have been proposed for the assessment of predictive efficiency in logistic regression have been detailed in the work of DeMaris.[14] Ultimately, the decision on the criteria for placing the separation lines will depend on the degree of confidence in the accuracy of the data and the cost of failure for a given scenario.

The consequences of failure and major failure are highly site-specific and the level of certainty required in a stable excavation must be determined by considering the cost of an unplanned failure or major failure. The consequences of misclassification and the probabilities of a given stability outcome determined from the isoprobability contours will depend on the data available. First, sufficient failure and major failure case studies must be available to define the stability zone boundaries accurately on the stability graph; and, second, adequate site-specific cases are required for accurate prediction of the consequences. The lower number of failure and major failure case histories compared with stable cases within the stability database causes a range of confidence in the accuracy of predicted stability zones. Fewer case histories reduce confidence in the results. Mining (with the exception of caving) is focused principally on the production of stable excavations. The stable zone on the stability graph is defined by the greatest number of case histories and, accordingly, our confidence is highest for designs that utilize this region of the stability graph.

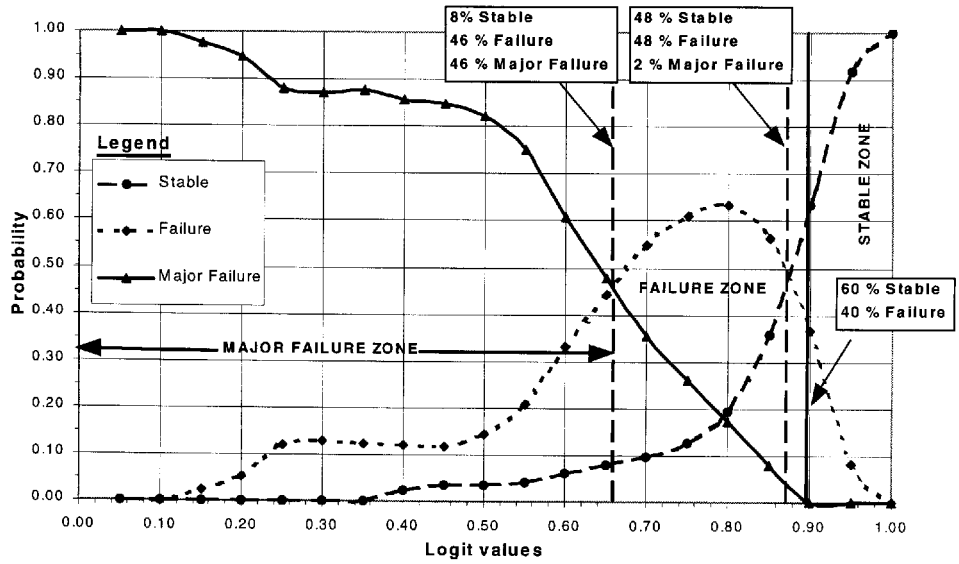

Fig. 7 Probability density functions for stability data determined from logit probability values

Size bias is an issue for the stable, failure and major failure classes within the stability database. Mining is focused on stability, so the imbalance in subset sizes mirrors the real distribution of stability cases within operational mines. The Mathews stability graph method is, moreover, a non-rigorous technique. The quality of the end-product—in this case a stability estimate (including probabilities)—can only be as good as the quality of the underlying data on which the method was formulated. One suggestion has been to apply a second optimization to consider size bias effects on the definition of the stability zones. This could be undertaken on a larger database and investigated by considering a random subsample from the stability database.

The logit model allows the direct effect of moving the stability zone boundaries to be quantified in terms of risk or probability of a specified stability outcome. Once a cost–risk

relationship has been developed for a site an appropriate level of risk can be determined and the stability zone boundaries and isoprobability contours on the Mathews graph can be tailored to the specific site. A cost–risk analysis is now possible and the optimal design limits can be chosen for individual operations.

Isoprobability contours

Although the stability zones can be defined statistically, a number of case histories report to the wrong zones. This is to be expected, given the inherent variability of rock masses, data that can be somewhat subjective and the fact that the design technique is non-rigorous. Diederichs and Kaiser[16] proposed the drawing of isoprobability contours to account for the uncertainties inherent in the design limits. Isoprobability contours allow the probabilities of stability, failure and major failure for a design surface to be obtained directly off the stability graph (an example is given in the Appendix).

The probability density functions have been determined

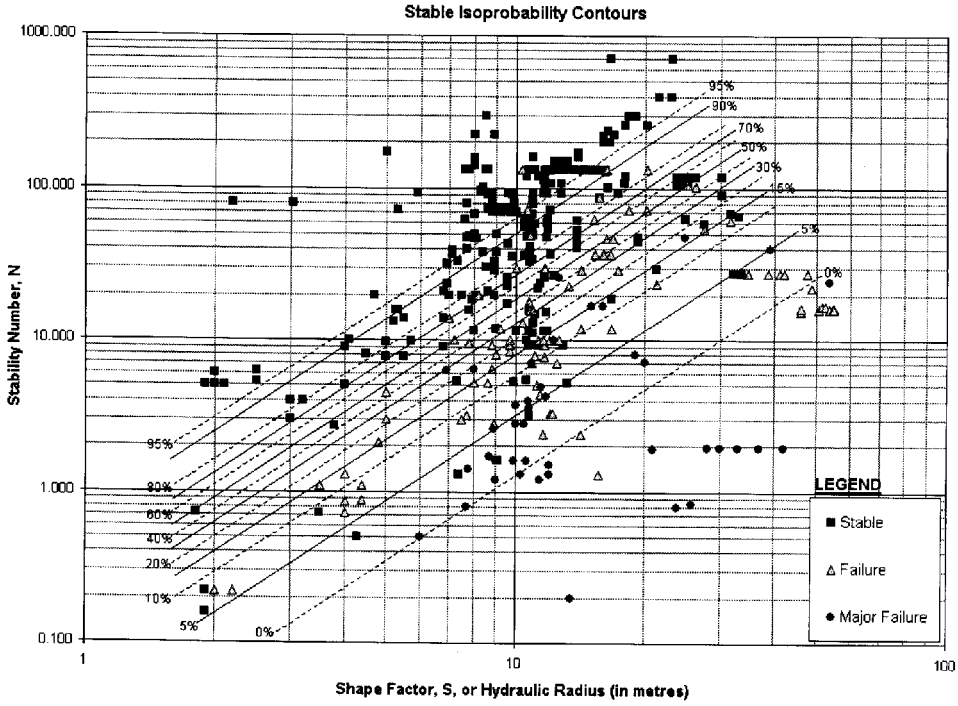

Fig. 8 Isoprobability contours for stable excavation based on logistic regression

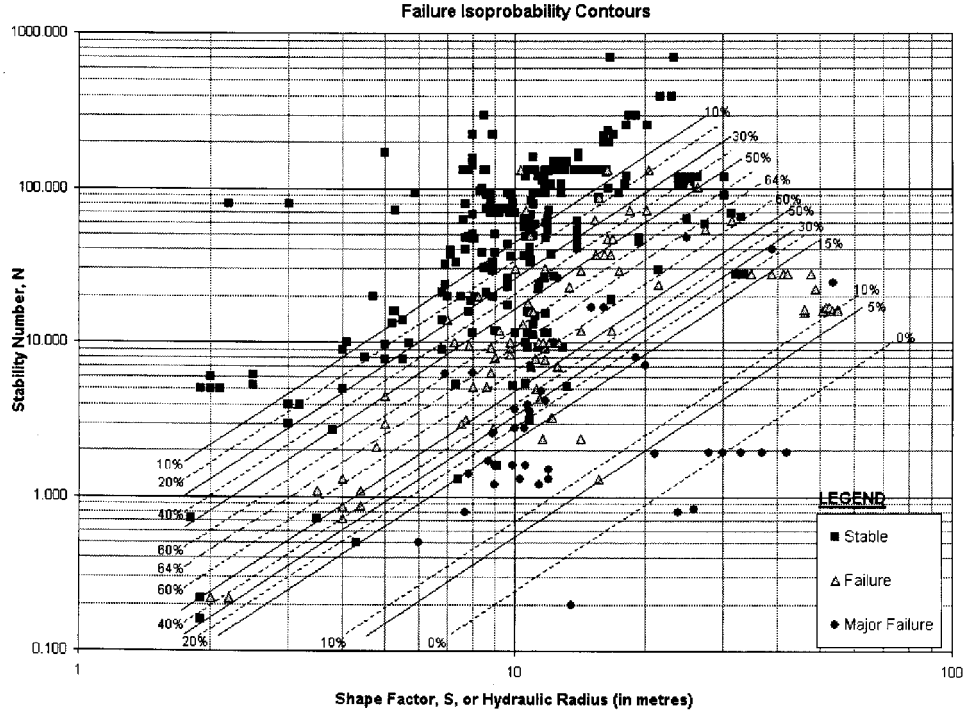

Fig. 9 Isoprobability contours for failure based on logistic regression

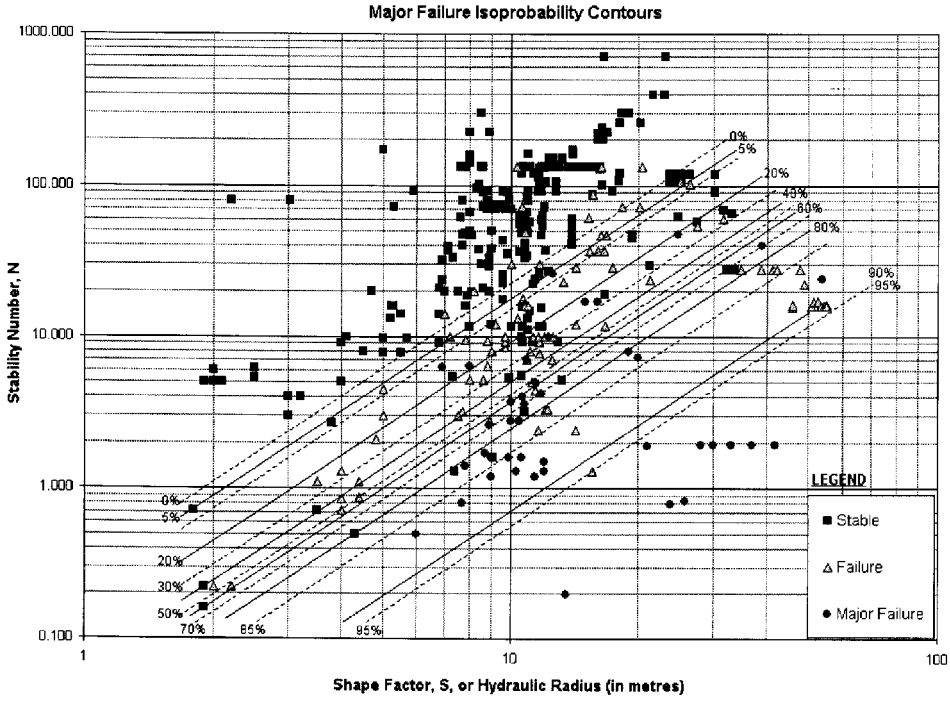

Fig. 10 Isoprobability contours for major failure based on logistic regression

for each of the stability classes (Fig. 7) from the predicted logit values. From the probability density functions the isoprobability contours were produced for the three separate levels of stability—stable (Fig. 8), failure (Fig. 9) and major failure (Fig. 10).

Accuracy and use of extended Mathews method

The Mathews stability graph encompasses a broad range of open-stoping experience and is essentially a self-validating model. Nevertheless, the validity and accuracy of the Mathews method depend on the quality and quantity of the stability data that it contains. The value of the documented stability data has been effectively increased by undertaking a least-squares regression to treat the uncertainties and subjectivity of the data.

The application of statistical methods in delineating stability zones and generating isoprobability contours has removed the subjectivity from the delineation of the zones. The application of regression techniques to a sufficiently large stability database is currently the best option for minimizing the influence of subjective data.

Major advantages of statistical determination of the zones on the stability graph are optimization of the design curves and the ability to evaluate the accuracy of the model. The precise nature of the risks associated with the position of the stability zone boundaries can be quantified. This removes the need for intermediate transition zones to be defined on the stability graph as general indicators of higher variability in the stability outcomes. Through the logit model the exact meaning of the stability zone boundaries, in terms of the probability of a given stability outcome, is precisely known.

Continual improvement of the accuracy of the model for all subsequent modifications is critical for optimization of the future use of the Mathews method in stope design. Through statistical techniques the value of the stability data can be maximized despite the inherent subjectivity. From the results objective interpretations can be made to improve what is acknowledged to be an empirical, non-rigorous, yet increasingly powerful design tool.

An example of how to use the Mathews stability graph method to assess the stability of an open stope is outlined in the Appendix.

Conclusions

The database for the Mathews method has been extended to more than 400 case histories, such that it now includes open-stoping experience for a broad range of surface geometries and rock mass conditions. The extended Mathews graph is a log–log plot with linear stable, failure and major failure zones rather than the traditional log–linear format with multiple curvilinear stability boundaries. The extension of the database has provided a wide-ranging data-set to which statistical methods can be applied.

Logistic regression was used to optimize the placement of stability zones and produce isoprobability contours for the prediction of stope surfaces that are stable or exhibit minor or major failures. The advantage of logistic regression lies in its ability to minimize the uncertainties reflected in the method through the use of maximum likelihood estimates.

The application of statistics does not change the subjectivity, degree of reliability or lack of rigour inherent in the Mathews method. Statistics can be used to take into account some of the inherent variability within the data, but the use of statistical regression must not be mistaken as adding a greater level of rigour to the Mathews stability graph method. Logistic regression should be viewed as an objective means to calculate zone boundaries and isoprobability contours for the available stability data. Through logistic regression the risks associated with using the technique can be quantified and the statistical significance of the stability zones becomes known.

The authors caution that both the Mathews stability graph method and subsequent statistical treatment rely on data that are not precise and care must be taken not to promote overconfidence in a result without recognizing the nature of the data underlying the method. The preferred approach to increasing the accuracy of the method is to increase the size and quality of the stability database and the authors are pursuing this.

The strength of the extended Mathews method lies in the

improved stability graph with statistically determined stability zone boundaries and isoprobability contours. The uncertainties inherent in the design technique can now be quantified over a larger range of stope surface geometries and rock mass conditions than was previously the case. This makes the extended Mathews method a powerful tool for risk assessment and optimization of open-stope design.

Acknowledgement

The work reported here is a component of research funded by the Australian Research Council. The authors thank Professor E. T. Brown for his review of the work.

References

1. Mathews K. E. *et al.* Prediction of stable excavation spans for mining at depths below 1000 m in hard rock. Report to Canada Centre for Mining and Energy Technology (CANMET), Department of Energy and Resources, 1980.
2. Barton N., Lien R. and Lunde J. Engineering classification of rock masses for design of tunnel support. *Rock Mechanics*, **6**, 1974, 189–236.
3. Bieniawski Z. T. *Engineering rock mass classifications: a complete manual for engineers and geologists in mining, civil, and petroleum engineering* (New York: Wiley, 1989), 251 p.
4. Potvin Y. Empirical open stope design in Canada. Ph.D. thesis, University of British Columbia, 1988.
5. Nickson S. D. Cable support guidelines for underground hard rock mine operations. M.App.Sc. thesis, University of British Columbia, 1992.
6. Hadjigeorgiou J., Leclair J. and Potvin Y. An update of the stability graph method for open stope design. Paper presented at CIM Rock Mechanics and Strata Control session, Halifax, Nova Scotia, 14–18 May, 1995.
7. Potvin Y., Hudyma M. R. and Miller H. D. S. Design guidelines for open stope support. *CIM Bull.*, **82**, no. 926, 1989, 53–62.
8. Stewart S. B. V. and Forsyth W. W. The Mathews method for open stope design. *CIM Bull.*, **88**, no. 992, 1995, 45–53.
9. Trueman R. *et al.* Experience in Australia with the Mathews method for open stope design. *CIM Bull.*, **93**, no. 1036, 2000, 162–7.
10. Laubscher D. H. A geomechanics classification system for the rating of rock mass in mine design. *Jl S. Afr. Inst. Min. Metall.*, **90**, 1990, 257–73.
11. Suorineni F. T., Tannant D. D. and Kaiser P. K. Fault factor for the stability graph method of open-stope design. *Trans. Instn Min. Metall. (Sect. A: Min. industry)*, **108**, 1999, A92–106.
12. Menard S. Applied logistic regression analysis (Beverley Hills: Sage, 1995), 98 p. *Sage University Paper Series on Quantitative Applications in the Social Sciences* no. 07-106
13. Liao T. L. Interpreting probability models: logit, probit, and other generalized linear models (Beverley Hills: Sage, 1984), 88 p. *Sage University Paper Series on Quantitative Applications in the Social Sciences* no. 07-101
14. DeMaris A. Logit modeling–practical applications (Beverley Hills: Sage, 1992), 87 p. *Sage University Paper Series on Quantitative Applications in the Social Sciences* no. 07-086
15. Holtsberg A. Stixbox—a statistics toolbox for Matlab and Octave. Logitfit.m, Lodds.m and Loddsinv.m. Available at http://www.maths.lth.se/matstat/stixbox/contents.html 1999 (cited 1/02/00)
16. Diederichs M. S. and Kaiser P. K. Rock instability and risk analyses in open stope mine design. *Can. Geotech J.*, **33**, 1996, 431–9.

Appendix

Using the Mathews stability graph method

The use of the stability graph for stability assessment in open-stope design is outlined here in an example from CSA mine in Cobar taken from the work of Stewart and Forsyth.[8] The example has been extended to illustrate the use of isoprobability contours in quantifying the uncertainty of stability within the stope design process.

An open stope is planned at a depth of 1000 m in an orebody that is 25 m wide and dips at 80°. Because of operational constraints the preferred stope length is 30 m and the stope height is 75 m. The geometry of the planned open stope is shown in Fig. 1 below.

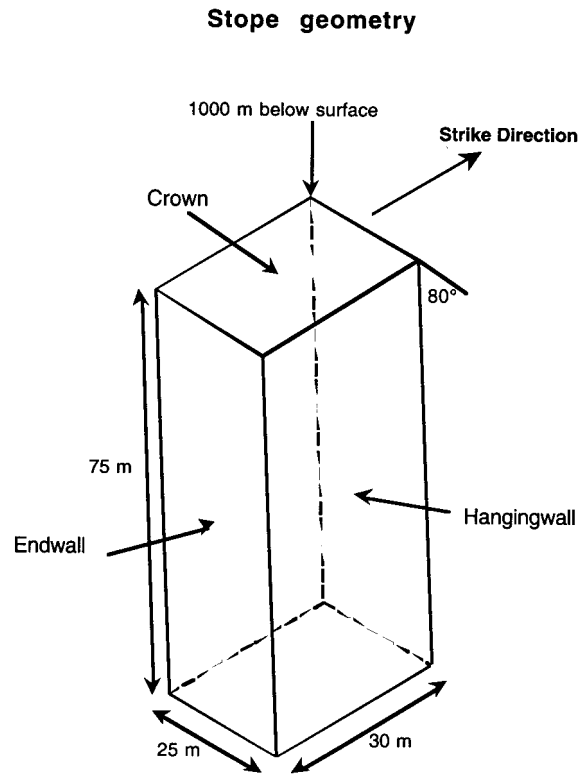

Fig. 1 Diagram of stope layout. After Stewart and Forsyth[8]

The average unconfined compressive strength of the intact rock is 120 MPa. The principal joint set is flat-dipping and closely spaced (average spacing is 10 cm). The joint surfaces are unaltered but display surface staining. Rock mass quality data have been collected and are summarized in Appendix Table 1 to the requirements of the NGI Q classification system.[2]

Table 1 Rock mass quality data used to determine Q' value

Item	Description	Value
Rock quality	Good	RQD = 85%
Joint sets	One joint set and random	$J_n = 3$
Joint roughness	Rough or irregular undulating	$J_r = 3$
Joint alteration	Unaltered with surface staining	$J_a = 1$

The first consideration when looking at the use of the Mathews stability graph in excavation design is to consider how current conditions compare with the data on which the technique was based. The non-rigorous and empirical nature of the Mathews method must be considered, and the strength and predictive capability of the method relies accordingly on the extent of the stability database: the method should not be used to predict stability outside the range of experience from which it was developed.

The first step in use of the Mathews method at the design stage is to determine the S and N values for each surface of the excavation. In this example four surfaces are examined—the footwall, hanging-wall, crown (or roof) and end-walls of the stope. As the principal joint set is flat-lying, the two end-walls of the stope are identical cases; however, if this were not so, the stability of each end-wall would need to be investigated separately.

Q' value

Application of equation 1 of the main text to the rock mass quality data in Table 1 yields a Q' value of 85.

Shape factor

The shape factor is the ratio of the area of the stope surface to the length of the perimeter of the surface. The S values calculated for the stope surfaces are given in Table 2.

Table 2 Calculated S values

Stope surface	Area, m²	Perimeter, m	Shape factor, S, m
Crown	750	110	6.8
Hanging-wall	750	210	10.7
Footwall	2250	210	10.7
Endwall	1875	200	9.4

Stress factor

To determine the stress factor for a surface the induced stresses at the mid-point of the surface must first be calculated. The induced stresses are rarely measured and thus must usually be estimated. If virgin *in-situ* stress measurements have been undertaken, these should be used as the basis for calculation of the induced stresses. If this is not the case, the *in-situ* stress state must be estimated from regional conditions. The induced stresses can be determined from elastic formulae, stress distribution plots, design curves or by running a simple elastic model in an appropriate numerical modelling package.

In this example the *in-situ* stresses have not been measured so the stress values must be estimated. As the stope is at a depth of 1000 m, the vertical stress is estimated to be 27 MPa. The ratio of the average horizontal to vertical stress, K, is estimated to be 1.4. This means that the average horizontal stress is calculated to be 38 MPa. The *in-situ* stresses used in determining the stress factor are shown in Fig. 2.

The next step, after estimation of the *in-situ* stresses before the stope is extracted, is to determine the induced stresses for each surface once the stope has been mined (Fig. 2). The magnitude of the induced stresses relative to the unconfined compressive strength of the rock is an important component of the stability assessment and is used to determine the rock stress factor.

Crown

Considering the top of the mid-stope vertical plane:

$\sigma_V = 27$ MPa; $\sigma_{H_2} = 38$ MPa
$K = \sigma_{H_2}/\sigma_V = 1.4$

Surface height = 75; Surface span = 25
Height to span ratio = 3

With a height to span ratio of 3 and a K value of 1.4 (from Fig. 3) σ_1/σ_V is estimated at 2.6. From this relationship it can be calculated that

$$\sigma_1 = 2.6 \times 27 = 70 \text{ MPa}$$

Once σ_1 is known the ratio of the unconfined compressive strength of the rock to the induced stresses can be calculated; in this case

$$\sigma_c/\sigma_1 = 120/70 = 1.7$$

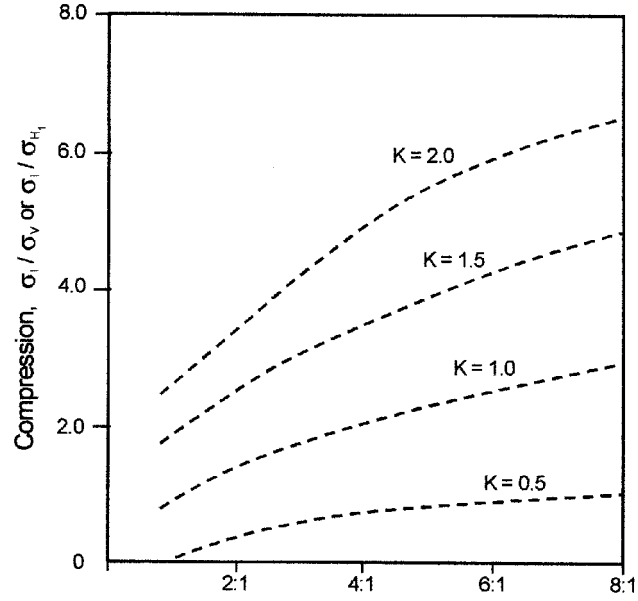

Fig. 3 Curves for estimation of induced stresses in backs and endwalls. After Stewart and Forsyth[8]

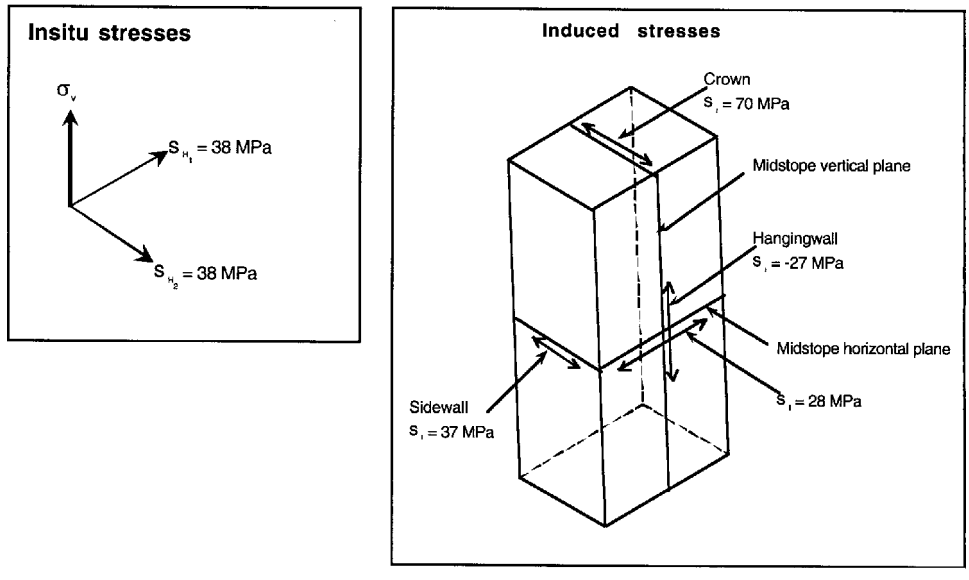

Fig. 2 *In-situ* (virgin) and induced stress diagrams showing mid-stope planes used to calculated rock stress factors for each surface. After Stewart and Forsyth[8]

The final stage in determining the magnitude of the stress factor consists in applying the value of σ_c/σ_1 to Fig. 2 and reading off the rock stress factor, which in this case is 0.1.

End-wall

Considering the strike end of the mid-stope horizontal plane:

σ_{H_1} = 38 MPa; σ_{H_2} = 38 MPa
$K = \sigma_{H_2}/\sigma_{H_1} = 1$

Surface height = 30; Surface span = 25
Height to span ratio = 1.2

For a height to span ratio of 1.2 and a K value of 1 σ_1/σ_{H_1} is estimated at 1.0 (from Fig. 3). Accordingly,

$\sigma_1 = 1.0 \times 38 = 38$ MPa

By reference to Fig. 2

$\sigma_c/\sigma_1 = 120/38 = 3.2$

and the rock stress factor for the end-wall is 0.25.

Hanging-wall and footwall

The next step is to determine the induced stresses in the hanging-wall and footwall considering the vertical and horizontal mid-stope planes. In the case where two estimates of the stress factor, A, are obtained (downdip and along strike) the lower value is used.

Considering the mid-stope vertical plane (downdip):

σ_V = 27 MPa; σ_{H_2} = 38 MPa
$K = \sigma_{H_2}/\sigma_V = 1.4$

Surface height = 75; Surface span = 25
Height to span ratio = 3

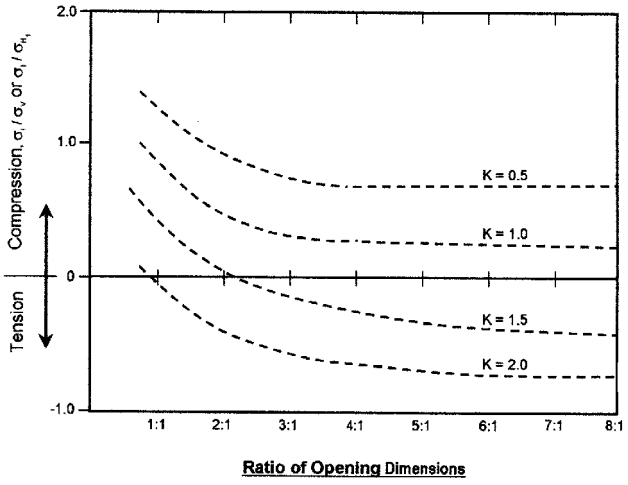

Fig. 4 Curves for estimation of induced stresses in hanging-walls. After Stewart and Forsyth[8]

For a height to span ratio of 3 and a K value of 1.4 (from Fig. 4) σ_1/σ_V is estimated at –0.1. As the value is negative, σ_1/σ_V is set to zero and σ_1 becomes zero. This makes σ_c/σ_1 greater than 10 and, therefore, the stress factor is equal to 1.

Note that the horizontal joints intersecting the hanging-wall will open because the induced stress at the centre of the hanging-wall span is tensile.

Considering the mid-stope horizontal plane (along strike):

σ_{H_1} = 38 MPa; σ_{H_2} = 38 MPa
$K = \sigma_{H_2}/\sigma_{H_1} = 1$

Surface height = 30; Surface span = 25
Height to span ratio = 1.2

For a height to span ratio of 1.2 and a K value of 1 σ_1/σ_{H_1} is estimated to be 0.75 (from Fig. 4). Accordingly,

$\sigma_1 = 0.75 \times 38 = 27.8$ MPa.

From Fig. 2

$\sigma_c/\sigma_1 = 120/27.8 = 4.3$

and the rock stress factor is 0.35.

The hanging-wall and footwall are both in compression in the direction of strike and in tension near the mid-span in the direction of dip. This gives two values on induced stress and two corresponding A values. Since the lower value is adopted, the rock stress factor for the hanging-wall and footwall of the stope is 0.35. The rock stress factors determined for each excavation surface are summarized in Table 3.

Table 3 Rock stress factors, A, determined for each excavation surface

Stope surface	A value
Crown	0.1
Hanging-wall	0.35
Footwall	0.35
End-wall	0.25

Joint orientation factor

The relative dip of the principal joint set and the excavation surface is used to determine the orientation factors (Table 4) for the individual surfaces (cf. Fig. 2). The principal joint set is defined as the feature that predominantly influences stability. In this case the dominant structure set has been identified as flat-dipping.

Table 4 B values

Stope surface	Orientation, degrees	B value
Crown	0	0.5
Hanging-wall	100	1.0
Footwall	80	1.0
End-wall	90	1.0

Surface orientation factor

The orientation of the stope surface influences the stability and, accordingly, a gravity adjustment factor, C (Table 5), is determined (cf. Fig. 2).

Table 5 C values

Stope surface	Dip of stope surface, degrees from horizontal	C value $C = 8 - 7 \cos$ (Dip from horizontal)
Crown	0	1
Hanging-wall	80	6.8
Footwall	+90	8.0
End-wall	90	8.0

Mathews stability number

The Mathews stability number for the exposed surfaces is determined from

$$N = Q' \times A \times B \times C$$

Table 6 N values

Stope surface	N value
Crown	4.3
Hanging-wall	200
Footwall	240
End-wall	170

Predicted stability outcome from stability graph

Once the shape factor and stability number are known the surfaces are plotted on the Mathews graph (Fig. 5). All the stope walls plot high in the stable zone, but the stope crown lies within the failure zone. This illustrates the quick, preliminary use of the stability chart; a more detailed assessment of the predicted risk of instability for each surface can be determined from isoprobability contours.

Estimation of probability of stability from isoprobability contours

Once the stability number and shape factor for the stope surfaces have been determined the probability of stability can be estimated from the plots of isoprobability contours for the

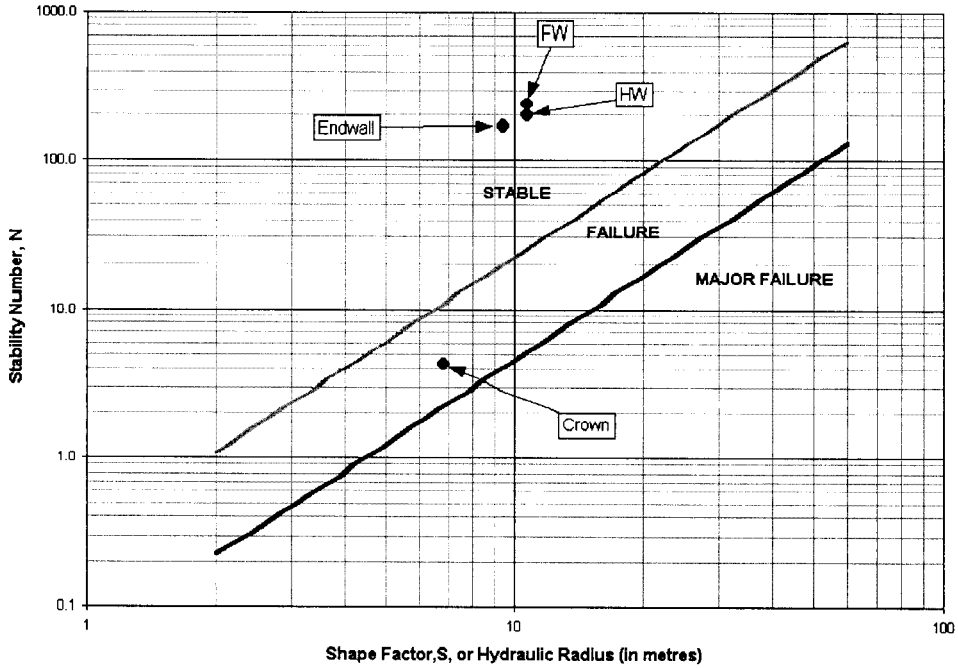

Fig. 5 Positions of surfaces can be plotted on stability graph to determine in which stability zones they lie

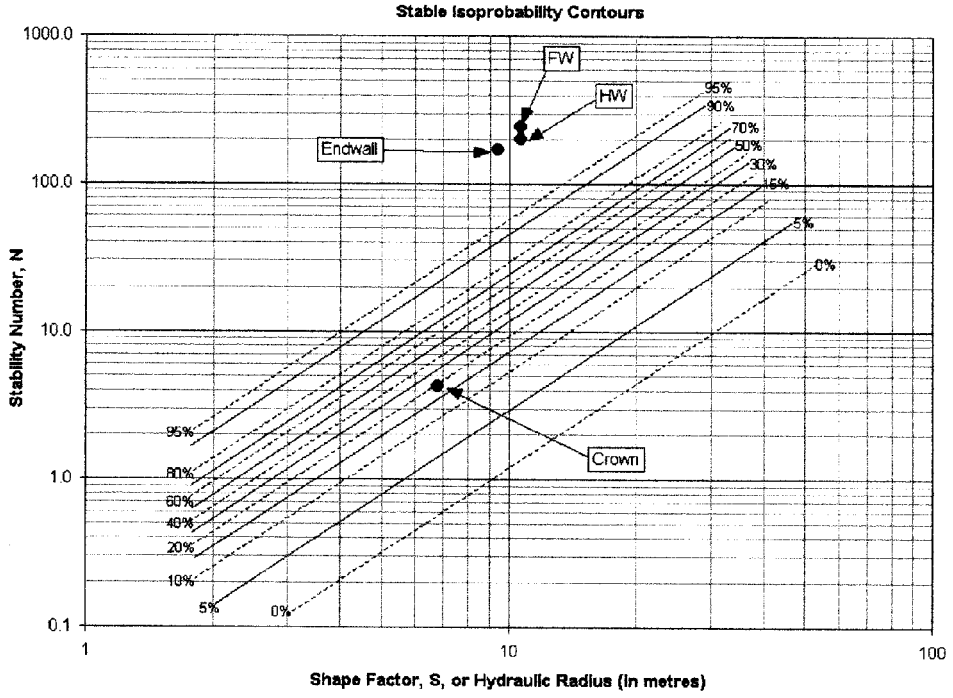

Fig. 6 Positions of surfaces can be plotted on stable isoprobability contours to determine probability of stope surface being stable

different stability outcomes. In this way a measure of the confidence in a stable estimate can be incorporated into the design process.

From consideration of the plotted position of the hanging-wall, footwall, end-wall and crown on the isoprobability contours in Figs. 8, 9 and 10 it is possible to estimate the probability of stability for the respective stope surfaces. The hanging-wall, footwall and end-walls have an estimated 100% probability of being stable (Fig. 6). In contrast, the crown of the stope has a high risk of failure—the surface has 18% probability of being stable, 64% probability of being a failure and 18% probability of being a major failure.

Discussion of probability results

For this example the stability of the stope walls is high. The predicted instability of the crown of the excavation is considerable and acceptability of the risk of failure of the crown will depend on the consequences of failure. The predicted cost and consequences of a crown failure are highly site-specific and should be developed from historical records for a given site.

The probabilities of instability determined for the crown can drive the design process in several directions. If 82% probability of failure or major failure is acceptable, the stope design can be implemented. If 82% probability of crown failure is unacceptable, the design of the stope needs to be readdressed. One option would be to reduce the stope height to lessen the roof stress or reduce the crown area. Previous experience will indicate whether a more conservative redesign of the stope or acceptance of the risk of crown failure is the better option in terms of safety, economic and operational issues. A second case may arise where the concern is not with failure but with a major failure in the crown. In this case the 18% probability of major failure may be unacceptable and could necessitate a redesign of the stope. This could be the case if a major failure were predicted to have consequences for the whole operation.

Conclusions

Knowing the probability of stability of a designed excavation allows the engineer to consider the level of risk that is acceptable on the basis of the probable extent and cost of failure. Estimation of the probabilities of stability enables a risk analysis to be undertaken, and if the cost of the varying degrees of failure can be approximated by reference to historical events, the design of the excavation can be optimized economically with true regard for the probability and cost outcomes.

Authors

C. Mawdesley graduated in geological engineering from the Royal Melbourne Institute of Technology. She has worked in mining geology, rock mechanics and mine planning, principally at Mount Isa Mines, Ltd. In 1998 she commenced Ph.D. studies in the field of block caving at the Julius Kruttschnitt Mineral Research Centre (JKMRC), University of Queensland, Australia.

Address: Julius Kruttschnitt Mineral Research Centre, Isles Road, Indooroopilly, Brisbane, Queensland 4068, Australia.

R. Trueman is currently Principal Research Fellow in mining at the JKMRC. He gained his Ph.D. in mining engineering from the University of Wales. He has worked previously as a rock mechanics engineer for the Anglo American Corporation in South Africa, as a production mining engineer for the National Coal Board and as senior lecturer in rock mechanics at the Camborne School of Mines in the United Kingdom and as research group manager for CSIRO Australia.

W. J. Whiten joined the JKMRC in 1966 and gained his Ph.D. in 1972 from the University of Queensland. He is currently Chief Scientist at the JKMRC.